EurJIC

European Journal of Inorganic Chemistry

Chemistry Europe

European Chemical Societies Publishing

Accepted Article

Title: Phosphine evaluation on a new series of heteroleptic copper(I) photocatalysts with dpa ligand [Cu(dpa)(P,P)]BF4

Authors: Marco A. Henriquez, Sebastian Engl, Pablo Jaque, Ivan A. Gonzalez, Mirco Natali, Oliver Reiser, and Alan R. Cabrera

To be cited as: *Eur. J. Inorg. Chem.* 10.1002/ejic.202100634

Link to VoR: https://doi.org/10.1002/ejic.202100634

WILEY-VCH

WILEY-VCH

FULL PAPER

Phosphine evaluation on a new series of heteroleptic copper(I) photocatalysts with dpa ligand [Cu(dpa)(*P,P*)]BF_4

Marco A. Henriquez,[a],[b] Sebastian Engl, [b] Dr. Pablo Jaque,[c] Dr. Ivan A. Gonzalez, [d] Prof. Dr. Mirco Natali, [e] Prof. Dr. Oliver Reiser,* [b] and Dr. Alan R. Cabrera* [a]

[a] Departamento de Química Inorgánica, Facultad de Química y de Farmacia, Pontificia Universidad Católica de Chile, Vicuña Mackenna 4860, Macul, Santiago, Chile. E-mail: arcabrer@uc.cl

[b] Institut für Organische Chemie, Universität Regensburg, Universitätsstrasse 31, Regensburg, Germany, Postal code 93053. E-mail: oliver.reiser@chemie.uni-regensburg.de

[c] Departamento de Química Orgánica y Fisicoquímica, Facultad de Ciencias Químicas y Farmacéuticas, Universidad de Chile, Sergio Livingstone 1007, 8380492, Santiago, Chile.

[d] Laboratorio de Química Aplicada, Instituto de Investigación y Postgrado, Facultad de Ciencias de la Salud, Universidad Central de Chile, Lord Cochrane 418, Santiago, Chile.

[e] Department of Chemical, Pharmaceutical and Agricultural Sciences (DOCPAS), University of Ferrara, Centro Interuniversitario per la Conversione Chimica dell'Energia Solare (SOLARCHEM), sez di Ferrara, Via L Borsari 46, 44121 Ferrara, Italy.

Abstract: Five new heteroleptic copper(I) complexes (**C1-5**) of the type [Cu(dpa)(*P,P*)]BF_4 based on dipyridylamine (dpa) as *N*,*N* ligand and commercial diphosphines as *P*,*P* ancillary ligands have been synthesised through a simple methodology with high yields. All complexes were thoroughly characterised by spectroscopic and spectrometric techniques, as well by theoretical calculations. These showed Metal to Ligand Charge Transfer (MLCT) absorptions in the 300–370 nm region, and emission in the 450–520 nm region with quantum yields and lifetimes that depend on the nature of the *P,P* ligand. The photocatalytic performance of copper(I) complexes **C1-5** was evaluated for their use as photoredox catalysts in ATRA reactions, decarboxylative coupling and an Appel-type reaction. The use of readily available dpa as *N*,*N* ligand constitutes an attractive alternative to the well-established phenanthroline ligands typically used in photocatalysis.

1. Introduction

One of the long-standing goals in organic chemistry has been the search for new synthetic routes that are sustainable, avoid toxic reagents, and exploit renewable energy sources in order to meet the requirements of green chemistry.[1] Within this context, a promising alternative to the thermal initiation of reactions has been the use of visible light as a mild and selective source for activating organic molecules.[2] However, most of the organic substrates only absorb in the ultraviolet (UV) region, and for this reason, photosensitizers and photoredox catalysts capable of absorbing energy in the visible region have been developed to trigger the desired reaction on given organic substrates. Ruthenium and iridium complexes have become the most popular photocatalysts due to their strong absorbance in the visible region, long excited state lifetime and high oxidation and reduction potentials that allow efficient energy or electron transfer to various organic substrates.[3] However, these metals are rare and expensive,[4] inspiring scientists to replace them with more abundant and environmentally friendly alternatives.[5] With this in mind, the use of copper complexes in photocatalysis has been recently developed by several groups, and especially, homoleptic copper complexes have been widely used for atom transfer radical additions (ATRA), allowing the difunctionalization of double bonds with various functionalities.[6]

Among the homoleptic Cu(I) complexes used, $[Cu(dap)_2]Cl$ (dap = 2,9-(*p*-anisyl)-1,10-phenanthroline)[7] has been arguably the most versatile, complying with the three key features of a suitable photocatalyst, i.e. absorbing in the visible range (437 nm), possessing a strong excited state reduction potential (–1.43 V vs. SCE), and a sufficiently long lifetime (270 ns in CH_2Cl_2) in the excited state to enable efficient bimolecular processes.[8] Nevertheless, the synthesis of the dap ligand requires several steps[8g-i] making readily available alternative desirable.[9]

Heteroleptic copper complexes have turned into a promising alternative due to their facile synthesis by ligand exchange with many commercially available bidentate *P,P* ligands.[10] Furthermore, their typical bulky structures provide substantial stability to the metal centre at the excited state level by preventing exciplex formation.[4, 11] Collins and coworkers have reported a library of heteroleptic complexes combining various bidentate *N,N*- and *P,P*-ligands.[12] In this way, effective photocatalysts both for single electron transfer (SET) and energy transfer (ET) processes could be identified for several photocatalytic reactions.[10a, 12-13] Likewise, other groups have reported several heteroleptic complexes capable of achieving C-C, C-Cl, C-S type couplings or exchange of functional groups. [14] Typically, the *N,N*-ligands used are based on the phenanthroline or bipyrdine core, representative examples are shown in Figure 1.

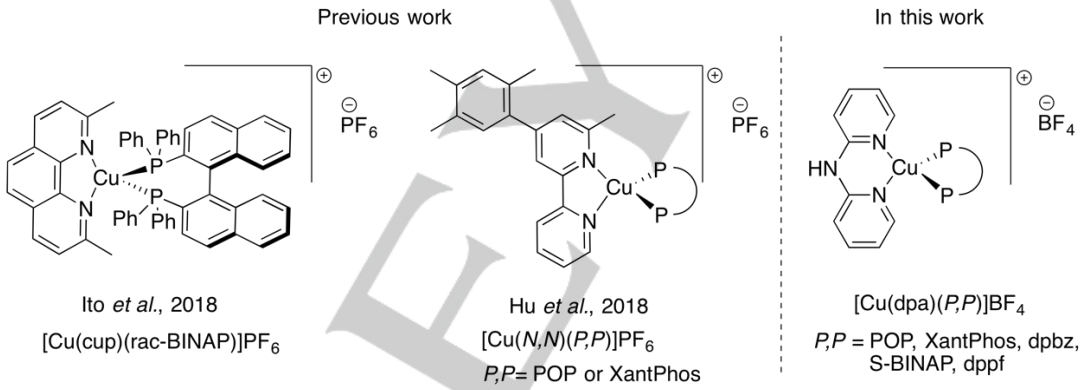

Figure 1. Heteroleptic Cu(I) photocatalyst.

In this work, we evaluate dipyridylamine (dpa) as a modular and readily available *N,N*-ligand in heteroleptic complexes with five commercial phosphines (POP, XantPhos, dpbz, dppf, S-BINAP) as potential photocatalysts, combining electrochemical and photophysical characterisation, density functional theory (DFT) together with time-dependent (TD-DFT) calculations, and applications in photoredox catalysis.

2. Results and Discussion

2.1. Synthesis and structural characterisation

Five new heteroleptic copper(I) complexes of the type $[Cu(dpa)(P,P)]BF_4$ were synthesised in two steps following methodologies reported in the literature (Scheme 1):[8c, 15] Equimolar amounts of dpa[16] ligand and $[Cu(CH_3CN)_4]BF_4$ were stirred in CH_2Cl_2 under N_2 atmosphere at 20 °C, followed by addition of the *P,P* ancillary

ligand. The resulting complexes were isolated by crystallization from CH_2Cl_2/toluene mixtures in 85–95 % yield, showing high air and thermal stability both in the solid-state as well as in solution for several days.

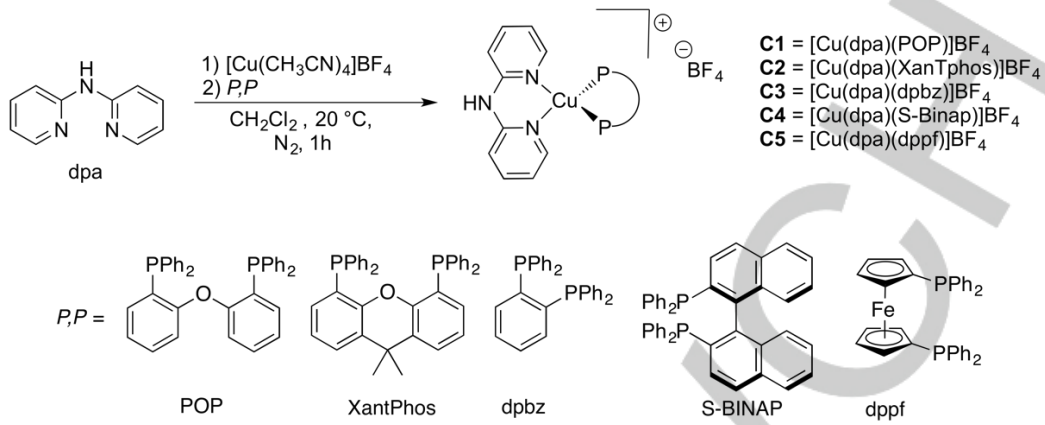

Scheme 1. Synthetic route to obtain heteroleptic Cu(I) complexes **C1-5**.

NMR characterisation of **C1-5** shows the successful coordination of the ligands to the metal centre as judged by the chemical shift in the ^{1}H spectra of N-H (close to 9.0 ppm) in all complexes compared to that of the dpa free ligand (close to 8.0 ppm). The phosphine signals in the ^{31}P NMR of all complexes exhibits a chemical shift compared to the free ligands and are observed in the range of 0 ppm to -14 ppm (see the ESI for the detailed characterisation).

The molecular structures of the complexes **C1-5** were obtained by XRD (Figure 2, Table 1). These complexes exhibit pseudo-tetrahedral coordination around the copper(I) mononuclear centre, surrounded by one dpa ligand and one bidentate phosphine ligand. The dpa ligands have small bite angles, in the range of 91°–94°, whereas the bidentate *P,P* ligands display larger bite angles, in the range of 100°–115°. The larger bite angle observed for XantPhos (**C2**) than for POP (**C1**) ligand can be attributed to the higher rigidity of the former due to the methylated cycloalkane. In general, the difference between the bite angles of the *N,N*, and *P,P* ligands induce the distortion observed to the tetrahedral geometry.

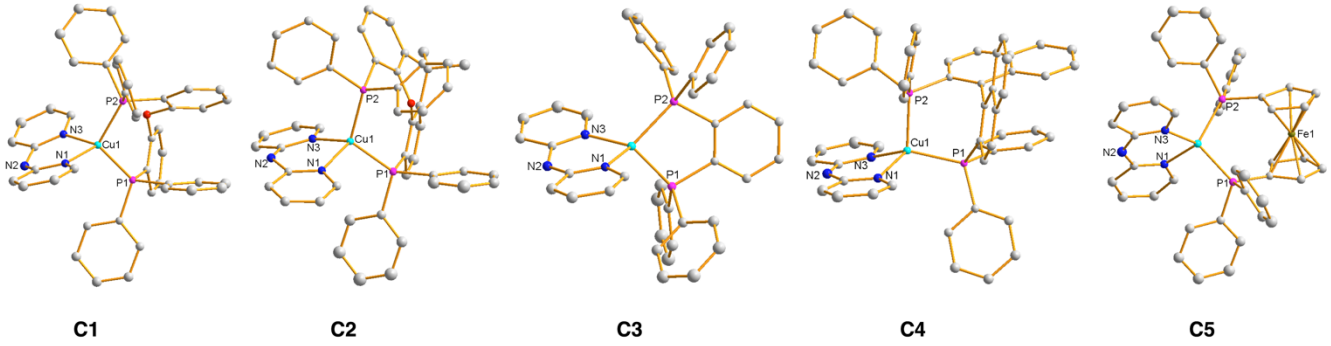

Figure 2. ORTEP plot of complexes **C1-5**, with partial numeration scheme. Hydrogen atoms and counter ion were removed for clarity. Thermal ellipsoids were drawn with 30 % probability

Table 1. Selected X-Ray analysis data for **C1-5.**

	C1	C2	C3	C4	C5
Bond Angle [deg]					
N1–Cu–N3	92.24	92.03	94.04	91.82	92.40
P1–Cu–P2	110.58	115.77	90.93	100.10	110.76
Dihedral Angle [deg]					
N1–Cu–N3 / P1–Cu–P2	89.47	88.69	80.57	82.50	78.38
Bond Length [Å]					
Cu–N1	2.039	2.051	2.018	2.059	2.061
Cu–N3	2.069	2.068	2.025	2.065	2.061
Cu–P1	2.270	2.254	2.249	2.265	2.279
Cu–P2	2.261	2.267	2.249	2.299	2.279

Based on the principal planes between the coordination atoms (N1–Cu–N3/ P1–Cu–P2), dihedral angles were calculated. From the point of view of the *P,P* ligand, the value is lower for the dppf ligand (**C5**) and larger for the POP ligand (**C1**), where the latter is close to the value expected for perpendicular planes. This suggests that the distortion from the tetrahedral geometry likely reflects the rigidity of the *P,P* ligand, where all values are similar to those reported in the literature for analogue complexes of the type [Cu(*N,N*)(*P,P*)]$^+$.[17] Regarding the bond distances, these are very similar among each complex. Small distances are observed between the nitrogen and the copper atoms (ca 2.05 Å), while longer lengths are seen for the Cu-P bond (in the range 2.24 Å – 2.29 Å), in agreement with values already reported.[18]

2.2. Electrochemical, photophysical and TD-DFT characterisation

The electrochemical properties of the complexes **C1-5** were measured by cyclic voltammetry (CV) in CH_2Cl_2 as solvent (Table 2, Figure S30). Complexes **C1**, **C2**, and **C4** exhibit one quasi-reversible oxidation process with a half-wave potential at ca 0.60 V vs. SCE, attributable to the Cu(I)/Cu(II) transition. For **C3**, this process occurs at less positive potentials (0.293 V vs. SCE) and is followed by an additional irreversible wave. The lower value for the Cu(I)/Cu(II) oxidation can be related to the reduced electron-withdrawing character of the diphosphine dpbz ligand as a consequence of the reduced bite angle imposed by the steric constrain of the ligand (*cf*. Table 1). In the case of **C5**, a reversible oxidation process is observed at $E_{1/2}$ = 0.88 V vs. SCE, followed by an intense and irreversible wave with a peak potential at 1.57 V vs. SCE. As observed for analogous Cu(I) complexes featuring a dppf ligand,[19] the first process can be assigned to oxidation of the ferrocenyl moiety. In contrast, the irreversible process at more positive potentials can be attributed to the oxidation of the copper metal centre, reflecting the electrostatic repulsion from the charged ferrocenyl moiety.[19] A comparison of the oxidation potentials of **C1-4** with those measured for the complexes reported by Hu and co-workers featuring a phenanthroline-based *N,N* ligand[14e] shows that the Cu(I) oxidation occurs at less positive values. This can be explained considering the influence of the dpa ligand being apparently less electron donating than polypyridine ligands.

Table 2. Summary of CV measurements, TD-DFT and excited state reduction potentials data of **C1-5.**

Complex	$E_{1/2}$ [a] [V]	E [eV]	λ [nm] (Character)	*f*	*P,P* bite angle [deg]	$[Cu^{I}]^*/[Cu]^{II}$ [c] [V]
C1	0.630	4.28 3.46	290 (LC+LLCT) 358 (MLCT, Cu→dpa)	0.0793 0.0526	110.58	-1.75
C2	0.690	4.37 3.50	284 (LLCT) 354 (MLCT, Cu→dpa)	0.0789 0.0509	115.77	-1.77
C3	0.293 0.785 [b]	4.24 3.28	293 (LC) 378 (MLCT, Cu→dpa)	0.1611 0.0456	90.93	-1.48
C4	0.550	4.35 3.56 2.99	285 (LLCT) 348 (MLCT, Cu→dpa) 415 (MLCT, dpaCu→P,P)	0.0912 0.0528 0.0308	100.10	-1.63
C5	0.881 1.575 [b]	4.36 3.58 2.41	284 (LC+LLCT) 354 (MLCT, Cu→dpa) 513 (d-dπ*)	0.0798 0.0233 0.0005	110.76	-1.88

[a] Cyclic voltammograms profiles recorded in anhydrous CH_2Cl_2 solution of **C1-5** (1 mM) with 0.1 M $TBAPF_6$ as supporting electrolyte at a scan rate of 0.1 V/s. Three-electrode cell configuration (Pt disc working electrode, saturated Ag/AgCl reference electrode and Pt wire counter electrode). $E_{1/2}$ values referred to SCE. [b] Irreversible wave, peak potential given. E = Electronic transition energy, λ = wavelength, *f* = oscillator strength. [c] Excited state reduction potentials were estimated via Rehm-Weller equation (see ESI).

The UV-Visible normalized spectra of the five heteroleptic Cu(I) complexes in CH_3CN as solvent are depicted in Figure 3. All the complexes showed intense absorption bands in the 200–300 nm region, plausibly attributable to spin-allowed π-π* ligand centred transitions. Additionally, weak and energetically lowest absorption bands between 300–370 nm are assignable to spin- allowed $d_{(Cu)}$-$\pi^*_{(N,N)}$ MLCT transitions involving the dpa ligand. Similar spectral patterns were observed in copper(I) complexes of the type $[Cu(NHC)(dpa)]^+$ reported by Costa's group.[16] Furthermore, **C5** exhibits a weak broader absorption band with a maximum at 440 nm, which can be assigned to Laporte forbidden d-d transitions involving the iron(II) centre of the dppf ligand (see ESI for more detail).

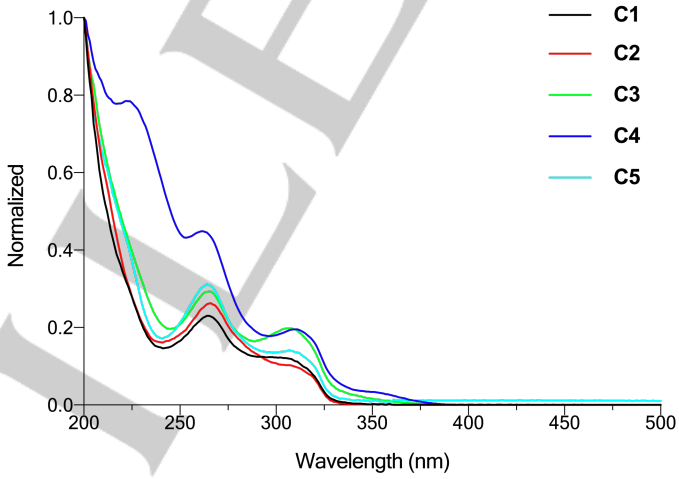

Figure 3. Normalized UV-Visible spectra for **C1-5** in CH_3CN at room temperature.

The vertical excited-states properties computed using the TD-DFT framework unveil the origin and the underlying electronic transitions in the complexes **C1-5**. The electronic transitions for **C1**, provided by TD-DFT calculations, are depicted in Figure 4 as a representative example, and the data for complexes **C1-5** are summarized in Table 2 and Table S1. Overall, it can be noted that the highest energy band is mainly dominated by the ligand-centred (LC) π-π* transition of the dpa ligand mixed, to a minor extent, with a ligand-to-ligand charge

transfer (LLCT) transition involving the dpa and *P,P* moieties. The weak band at lower energy is mainly characterised by metal-to-ligand charge transfer (MLCT) transition from Cu(I) to dpa ligand (*cf.* Table 2). However, one exception to this general behaviour is found, specifically, in **C4**. In this case, an additional MLCT band at lower energy is observed, where its character involves a charge transfer from the dpa-Cu(I) fragment to the *P,P* ligand (See Figure S31).

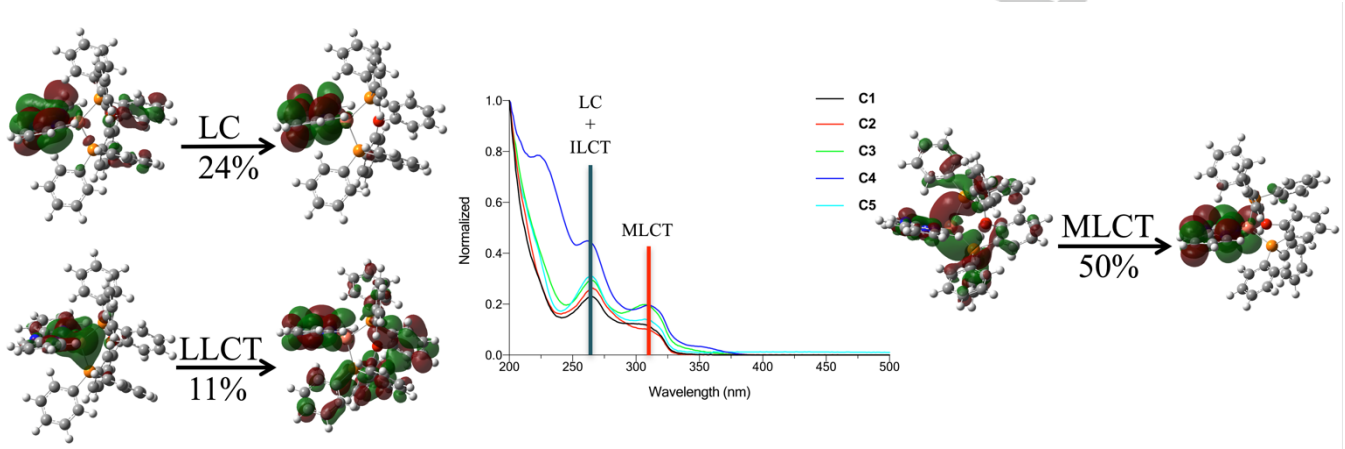

Figure 4. Electronic transitions character for **C1**, obtained by TD-DFT calculations.

The photoluminescence properties of all complexes were studied in degassed CH_2Cl_2 solution at room temperature and 77 K in a 4/1 ethanol/methanol glassy matrix (Table 3, Figure 5). All complexes **C1-5** exhibit emission in CH_2Cl_2 at room temperature (Figure 5a). Quantum yields of 3.1 % and 1.9 % were measured for **C1** and **C2**, respectively, whereas quantum yields <0.1 % were recorded for the remaining complexes (see Table 3). Lifetimes of 8.6, 7.9, and 20.8 µs were measured for **C1**, **C2**, and **C4**, respectively, while for the other complexes, the lifetimes were below the instrumental resolution (<10 ns). The nature of the emissive state can be discussed in relation to the luminescence spectra measured at 77 K (Figure 5b). Complexes **C1**, **C2**, **C3**, and **C5** show an emission which undergoes a substantial blue-shift when recorded in the glassy matrix at 77 K. This can be attributed to the rigidochromic effect exerted by the solid-state matrix and is characteristic of excited states of charge transfer nature. Accordingly, the corresponding luminescence can be attributed to phosphorescence from a triplet MLCT involving a formal Cu(II) centre and a reduced dpa ligand. However, the appreciably long lifetime observed in **C1-3** at 77 K (hundreds µs, Table 3) strongly suggests that contribution of a triplet LLCT state cannot be completely ruled out.[20] This attribution agrees with the trend in the energy of the luminescence maxima that reflects the observed trend in the oxidation potential of the Cu(I) centre. Furthermore, these considerations well comply with the quantum yield and lifetime data measured at room temperature for complexes **C1** and **C2** and the corresponding radiative constants (~$3x10^4$ s^{-1}), whose values are in the order of those found for similar copper(I) complexes.[21] On the other hand, both reduced quantum yields and lifetimes for complexes **C3** and **C5** seem to be characteristic of these types of complexes and thus correlate with the nature of the *P,P* ligand. For **C3**, the small P–Cu–P angle (~90°) and smaller dihedral angle (see Table 1) very likely promote efficient flattening distortion within the excited state, thus improving non-radiative deactivation routes. On the other hand, in **C5**, the ferrocenyl moiety within the dppf ligand is expected to quench the triplet MLCT excited state via energy transfer.[19] This

quenching process maintains its intrinsic efficiency in the glassy matrix at 77 K, thus explaining the short lifetime measured for **C5** also under these latter conditions.

Table 3. Summary of emission properties of **C1-5**.

	CH_2Cl_2			77 K	
	λ [nm]	Φ [%]	τ [μs]	λ [nm]	τ [ms]
C1	520	3.1 [a]	8.6	453	0.46
C2	504	1.9 [a]	7.9	455	0.41
C3	590	0.08 [b]	- [d]	507	1.6
C4	567	0.09 [b]	20.8	500,539,581,634	15.1
C5	449	0.02 [c]	- [d]	380, 399, 420	- [d]

[a] using fluoresceine in 0.1 M NaOH (Φ = 0.94) as the standard. [b] using $Ru(bpy)_3^{2+}$ in H_2O (air-equilibrated, Φ = 0.028) as the standard. [c] using quinine sulfate in 0.05 M H_2SO_4 (Φ = 0.53) as the standard. [d] below the detection limit of the laser flash photolysis (ca 10 ns).

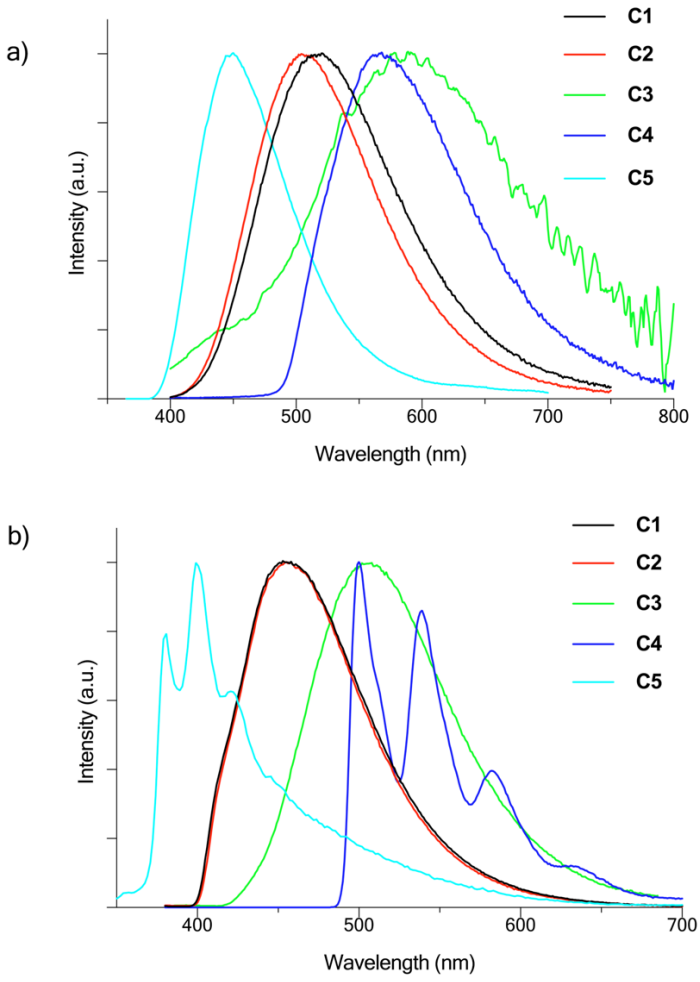

Figure 5. Emission spectra of **C1-5** in a) N_2-purged CH_2Cl_2 at room temperature and b) 4/1 ethanol/methanol glassy matrix at 77 K

The emission of complex **C4** at 77 K occurs at similar energies as observed at room temperature. It displays a structured profile with three distinct maxima suggesting a different character of the emitting excited state with respect to the other Cu(I) complexes of the series. Interestingly, this phosphorescence is similar to that found for a related $Cu(BINAP)_2^+$ complex[22] and can be assigned to a triplet LC involving the binaphthyl group of the *P*,*P* ligand.

The observed long lifetime (15.1 ms), characteristic of spin-forbidden deactivation from LC excited states, is entirely consistent with this attribution. An emitting state of LC character even in CH_2Cl_2 at room temperature well explains the small quantum yield experimentally measured. The latter, combined with the lifetime of 20.8 µs, indeed provides a radiative constant of 43 s^{-1}, which is considerably smaller than that calculated for the triplet MLCT state in complexes **C1** and **C2** (see above) and thus consistent with the different nature of the excited state in **C4** responsible for the observed luminescence.

2.3. Photocatalytic studies

To study the photocatalytic activity of the synthesised complexes, the ATRA reaction between styrene (**1**) and CBr_4 (**2**) was chosen as the model reaction (Table 4). Importantly, the desired product **3** is not obtained by omitting the catalyst (Table 4, entry 1). Established Cu-photocatalysts like $[Cu(dap)_2]Cl$ or [Cu(cup)(*rac*-BINAP)]PF_6 are capable of delivering the **3** in good to excellent yields (Table 4, entries 2-3). Hence, we subjected the complexes **C1-5** to the reaction (entries 4-8), which revealed that **C4** indeed a competent catalyst in the title reaction, giving rise to **3** in excellent yield of 99 % (Table 4, entry 7). Notably, this reaction can also be scaled to gram-quantities of product (Scheme 2, A) showcasing the viability of the catalyst for preparative purposes. In line with the observed electrochemical and photophysical properties (Table 2 and 3), the improved activity of complex **C4** is associated with S-BINAP as the *P,P* ancillary ligand which confers rigidity to the complex. As a consequence, a long excited-state lifetime arises, which seems to be pivotal in favouring enhanced photocatalytic activity via bimolecular routes. No asymmetric induction in **3** was observed, suggesting that the introduction of the CBr_3 group into the product does not benefit from the chiral nature of catalyst **C4**.

Table 4. ATRA test reaction evaluation using **C1-5**.[a]

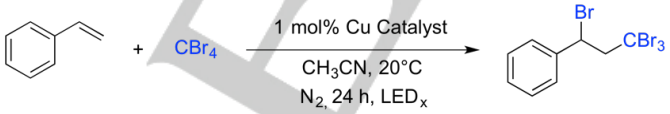

Entry	Catalyst	LED_x	Yield % [b]
1	without	455	n.r
2	$Cu(dap)_2Cl$	530	99
3	[Cu(cup)(*rac*-BINAP)]PF_6	455	71[9]
4	[Cu(dpa)(POP)]BF_4 (**C1**)	455	37
5	[Cu(dpa)(XantPhos)]BF_4 (**C2**)	455	15
6	[Cu(dpa)(dpbz)]BF_4 (**C3**)	455	51
7	[Cu(dpa)(S-BINAP)]BF_4 (**C4**)	455	99
8	[Cu(dpa)(dppf)]BF_4 (**C5**)	455	15

[a] styrene (0.5 mmol, 1.0 equiv), CBr_4 (0.5 mmol, 1.0 equiv), catalyst (1 mol%) in CH_3CN (dry, degassed, 3 mL); Irradiation at X nm (LED) under N_2 atmosphere for 24 h at 20 °C. [b] ^{1}H-NMR Yield was determined using 1,3,5-trimethoxybenzene as an internal standard.

Further utilisation of **C4** in other types of photochemical reactions was investigated (Scheme 2). Chlorosulfonylation of styrene was achieved in 93 % similar to the previous report by $[Cu(dap)_2]Cl$ (96 %).[9] Again scale-up of the transformation is possible accessing gram-amounts of **6** with only a small decrease in reaction yield. Remarkably, subjecting alkynes to the chlorosulfonylation reaction, the selective formation of the E isomer is observed in good yields (**7a-7c**), contrasting $[Cu(dap)_2]Cl$ which produces *E/Z* mixtures of products. It is assumed that Cu(*N,N*)(*P,P*)$^+$ complexes are able to promote an additional energy transfer pathway to convert the Z product

to the corresponding *E* isomer, which is in accordance to recent reports by Hu and coworkers[23] and Collins and coworkers.[24] **C4** was moderately effective in the visible-light Appel-type reaction (Scheme 2, C), converting alcohol **8** to halide **9** in 56 % yield, which nevertheless constitutes a higher yield compared to $[Cu(dap)_2]Cl$ (40 %).[9] Finally, *N*-(acyloxy)phtalimides derivatives have been used as radical source in carbon-carbon bond forming processes for several groups.[25] Indeed, **C4** achieved the decarboxylative fragmentation of **10** and subsequent coupling with **11** to access C_{sp3}-C_{sp} coupling product **12** in 52 % yield, comparable to other heteroleptic Cu(I) photocatalysts reported by Collins in 2018.[12]

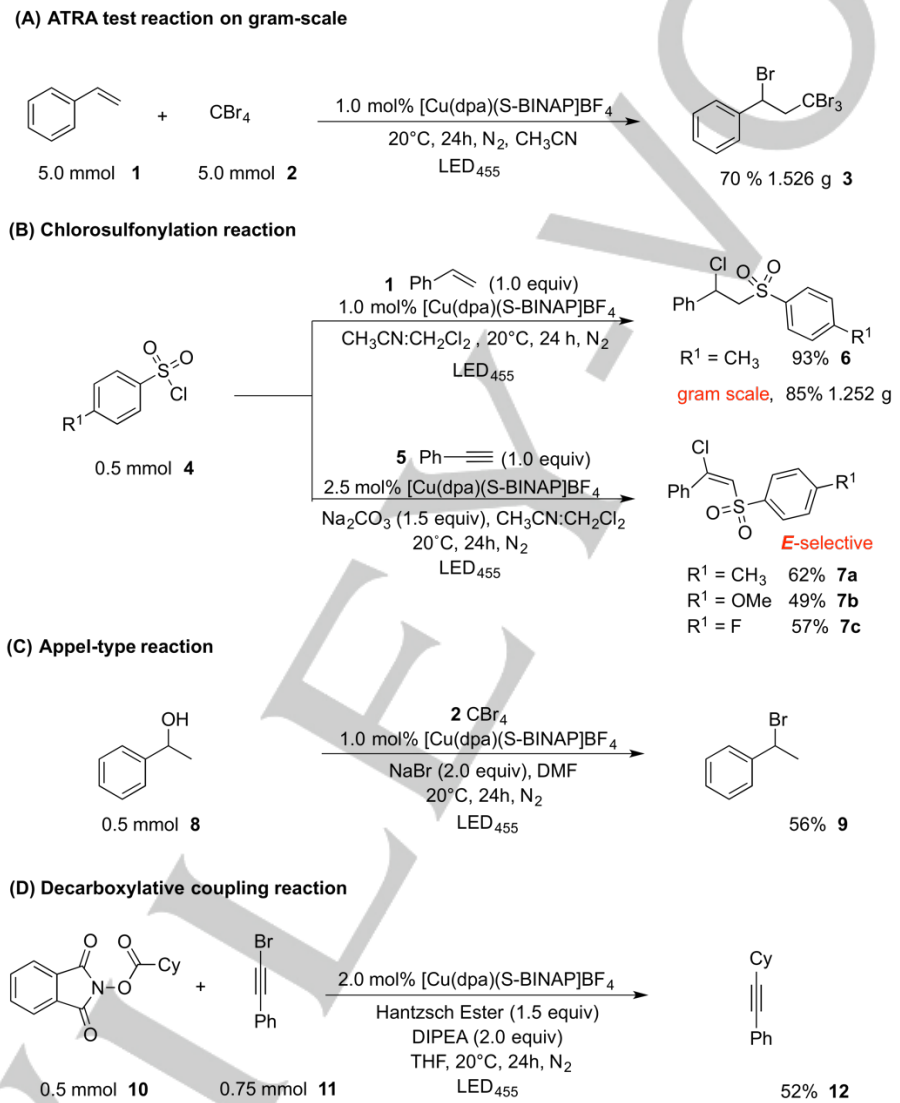

Scheme 2. (A) ATRA test reaction on gram scale. Use of $[Cu(dpa)(S\text{-}BINAP)]BF_4$ in different photo-redox reactions. (B) Chlorosulfonylation reaction (C) Appel-type reaction (D) Decarboxylative coupling reaction. For more details see ESI.

3. Conclusion

Five new heteroleptic Cu(I) complexes containing dpa *N,N* ligand and *P,P* auxiliary ligand have been successfully synthesised, with yields between 85–95 %, and structurally characterised by NMR, FT-IR, HRMS, and XRD. All

structural characterisations are in agreement with the formation of mononuclear heteroleptic complexes. The electrochemical and optical characterisation have been examined, and TD-DFT calculations supported and assigned the character of observed UV-Vis bands. **C1-5** exhibited redox potentials in the range 0.293–1.575 V v/s SCE, MLCT band centred around 300–370 nm, and excited-state lifetimes of 8.6–20.8 μs. The longer lifetime that has been observed for **C4** is pivotal towards profitable photocatalytic applications as demonstrated for five representative transformations, rivalling other homo- and heteroleptic Cu(I)-photocatalysts with respect to versatility and efficiency. Given the facile availability of the dipyridylamine (dpa) on multigram scale, this ligand appears to be an attractive alternative to the more established *N,N*-dimine and in particular to the widely used 2,9-*p*-anisyl-phenanthroline (dap) ligand.

4. Experimental Section

All reagents were purchased from commercial sources, unless otherwise specified and used as received. Based on the methodology reported by Sekar *et al*.[26] we developed a new synthetic route to obtain *N,N* dpa ligand in higher yields (81 %). For more details, see ESI. NMR spectra were recorded on NMR Bruker AV 400 MHz and AV 300 MHz. Chemical shifts are given in parts per million relatives to TMS (^{1}H and ^{13}C, δ($SiMe_4$) = 0). Most NMR assignments were supported by additional 2D experiments. HRMS-ESI-MS experiments were carried out using a Thermo Scientific Exactive Plus Orbitrap Spectrometer. FT-IR spectra were recorded on a Bruker Vector 22 Spectrophotometer using Merck GF-254 type 60 silica gel. Column chromatography was carried out using Merck silica gel 60 (70–230 mesh). The cyclic voltammograms were recorded using a PalmSens 3 Instruments Potentiostat, a platinum disc working electrode with an area of 0.02 cm^2, a saturated Ag/AgCl reference electrode and a platinum wire counter electrode. All electrochemical measurements were carried out in anhydrous dichloromethane solutions of Cu(I) complexes (1 mM) with tetrabutylammonium hexafluorophosphate ($TBAPF_6$) (0.1 M) as the supporting electrolyte at a scan rate of 0.1 V s^{-1}. UV-Vis absorption spectra were recorded on a Jasco V-570 UV/Vis/NIR spectrophotometer. Photoluminescence spectra were taken on an Edinburgh Instrument spectrofluorometer. Emission lifetimes were taken on a laser flash photolysis apparatus comprised of a Continuum Surelite II Nd:YAG laser (excitation at 355 nm, FWHM = 6–8 ns, was provided by THG from the 1064-nm fundamental). Light emitted by the sample was focused onto the entrance slit of a 300 mm focal length Acton SpectraPro 2300i triple grating, flat field, and double exit monochromator equipped with a photomultiplier detector (Hamamatsu R3896). Signals from the photomultiplier were processed by means of a TeledyneLeCroy 604Zi (400 MHz, 20 GS/s) digital oscilloscope. CH_2Cl_2 solutions of metal complexes **C1-5** were purged using nitrogen gas for 20 minutes before steady-state and time-resolved emission measurements. Single-crystal X-ray diffraction data were recorded on an Agilent Technologies SuperNova diffractometer with Cu Kα radiation (λ = 1.54184 Å). Crystals were selected under mineral oil, mounted on MicroMount loops, and quench-cooled using an Oxford Cryo-system open flow N_2 cooling device. The structure was solved with the ShelXT[27] structure solution program using the dual solution method and by using Olex2[28] as the graphical interface. The model was refined with version 2018/3 of ShelXL[29] using Least Squares minimisation. Full details can be found in the independently deposited crystallography information files (cif), CCDC numbers: 2098431 for **C1**, 2098436 for **C2**, 2098449 for **C3**, 2098451 for **C4**, and 2098493 for **C5**.

4.1. Synthesis of the compounds

General synthetic procedure of complexes: dpa ligand (1.0 equiv) in CH_2Cl_2 was added dropwise to a solution of $[Cu(CH_3CN)_4]BF_4$ (1.0 equiv) in CH_2Cl_2 under nitrogen atmosphere. The reaction mixture was stirred for 30 minutes at 20 °C. After this time, a diphosphine ligand (1.0 equiv) solution in CH_2Cl_2 was added dropwise to the reaction mixture and stirred for additional 30 minutes. Finally, the solvent was removed under vacuum, and the crude product was purified by crystallization using a CH_2Cl_2/Toluene mixture at -20 °C.

Complex C1: Isolated as white powder in 85 % yield (853.2 mg, 0.992 mmol). ^{1}H-NMR (400 MHz, $CDCl_3$, 298 K): δ/ppm = 9.0 (s,1H, N-H), 7.70 (dd, *J* = 5.7 Hz, 1.7 Hz, 2H), 7.50 (ddd, *J* = 8.9 Hz, 7.2 Hz, 1.9 Hz, 2H), 7.36 (d, *J* = 8.3 Hz, 2H), 7.34–7.26 (m, 6H), 7.23 (t, *J* = 7.5 Hz, 8H), 7.13 (dt, *J* = 7.1 Hz, 5.0 Hz, 8H), 7.06–6.98 (m, 4H), 6.91–6.85 (m, 2H), 6.48 (t, *J* = 6.4 Hz, 2H). ^{13}C{^{1}H} NMR (100 MHz, $CDCl_3$, 298 K): δ/ppm = 157.8 (t, J^{C-P} = 6.2 Hz), 153.8, 147.1, 138.7, 134.3, 133.2 (t, J^{C-P} = 8.2 Hz), 131.7, 131.1 (t, J^{C-P} = 16.0 Hz), 129.9, 128.7 (t, J^{C-P} = 4.7 Hz), 125.0, 124.6 (t, J^{C-P} = 13.1 Hz), 120.1, 116.8, 115.8. ^{19}F NMR (400 MHz, $CDCl_3$, 298 K): δ/ppm = -151.17 (s, BF_4), ^{11}B NMR (128 MHz, $CDCl_3$, 298 K): δ/ppm = -0.64 (s, BF_4). ^{31}P(1H) (160 MHz, $CDCl_3$, 298 K): δ/ppm = -13.37 (s, POP). HRMS (ESI): m/z [M]+ for $C_{46}H_{37}CuN_3OP_2$: Calculated = 772.1758, Found = 772.1758.

Complex C2: Isolated as white powder in 90 % yield (946.3 mg, 1.05 mmol) ^{1}H-NMR (400 MHz, CD_2Cl_2, 298 K): δ/ppm = 8.85 (s, 1H, N-H), 7.65 (dd, J = 7.8 Hz, 1.4 Hz, 2H), 7.52 (ddd, *J* = 8.8 Hz, 7.2 Hz, 1.9 Hz, 2H), 7.42 (dd, *J* = 5.6 Hz, 1.2 Hz, 2H), 7.31 (t, *J* = 7.3 Hz, 4H), 7.24 (m, 4H), 7.17 (m, 20H), 6.55 (m, 2H), 6.42 (m, 2H), 1.76 (s, 6H). ^{13}C{^{1}H} NMR (100 MHz, CD_2Cl_2, 298 K): δ/ppm = 155.3 (t, J^{C-P}= 6.3), 154.2, 147.5, 139.6, 138.5, 134.0 (t, J^{C-P}= 1.6), 133.64 (t, J^{C-P}= 8.1), 132.5 (t, J^{C-P}= 16.1), 131.55, 130.46, 129.5, 129.3 (t, J^{C-P}= 4.7), 128.72, 127.44, 125.8, 125.64 (t, J^{C-P}= 2.4), 121.14 (t, J^{C-P} = 12.8), 117.53, 116.10, 28.20. ^{19}F NMR (400 MHz, CD_2Cl_2, 298 K): δ/ppm = -150.61 (s, BF_4). ^{11}B NMR (128 MHz, CD_2Cl_2, 298 K): δ/ppm = -0.79 (s, BF_4). ^{31}P(^{1}H) NMR (160 MHz, CD_2Cl_2, 298 K): δ/ppm = -13.15 (s, XantPhos). HRMS (ESI): m/z [M]+ for $C_{49}H_{41}CuN_3OP_2$: Calculated = 812.2021, Found = 812.2075.

Complex C3: Isolated as white powder in 86 % yield (771.5 mg, 1.00 mmol) ^{1}H-NMR (400 MHz, $CDCl_3$, 298 K): δ/ppm = 9.00 (s, 1H, N-H), 7.55 (m, 4H), 7.49 (m, 2H), 7.23 (m, 26H), 7.02 (m, 2H), 6.90 (m, 2H), 6.42 (m, 2H). ^{13}C{^{1}H} NMR (100 MHz, $CDCl_3$, 298 K): δ/ppm = 153.7, 147.8, 141.6 (t, JC-P = 33.6 Hz), 137.0, 135.0, 132.82–132.3, 131.2, 130.2, 129.9, 129.0 (t, JC-P = 4.7 Hz), 116.4, 115.8. ^{19}F NMR (400 MHz, $CDCl_3$, 298 K): δ/ppm = -151.25 (s, BF_4), ^{11}B NMR (128 MHz, $CDCl_3$, 298 K): δ/ppm = -0.67 (s, BF_4). ^{31}P(^{1}H) NMR (160 MHz, $CDCl_3$, 298 K): δ/ppm = -7.06 (s, dpbz). HRMS (ESI): m/z [M]+ for $C_{40}H_{33}CuN_3P_2$: Calculated = 680.1446, Found = 680.1490.

Complex C4: Isolated as green powder in 92 % yield (1.04 g, 1.07 mmol) ^{1}H-NMR (400 MHz, $CDCl_3$, 298 K): δ/ppm = 8.75 (s,1H, N-H), 7.79 (dd, *J* = 5.5 Hz, 1.8 Hz, 2H), 7.62–7.48 (m, 6H), 7.45–7.40 (m, 4H), 7.35–7.27 (m, 6H), 7.26–7.18 (m, 6H), 6.91 (t, 2H, *J* = 7.7 Hz), 6.82–6.75 (m, 4H), 6.70 (t, 2H, *J* = 6.3 Hz), 6.65 (t, 2H, *J* = 7.5 Hz), 6.53 (d, 2H, *J* = 8.6 Hz), 6.49–6.44 (m, 4H). ^{13}C{^{1}H} NMR (100 MHz, $CDCl_3$, 298 K): δ/ppm = 154.8, 147.7, 139.5, 139.4, 134.4 (t, J^{C-P} = 9.7 Hz), 133.8 (t, J^{C-P} = 4.0 Hz), 133.1, 132.9 (t, J^{C-P} = 8.7 Hz), 132.2–131.8, 130.5, 129,7, 129.3–129.1, 128.9, 127.9, 127.6 (t, J^{C-P} = 5.1 Hz), 127.2, 126.8, 126.7, 126.5, 117.5, 116.5. ^{19}F NMR (400 MHz, $CDCl_3$, 298 K): δ/ppm = -151.13 (s, BF_4). ^{11}B NMR (128 MHz, $CDCl_3$, 298 K): δ/ppm = -0.70 (s, BF_4). ^{31}P(^{1}H) NMR

(160 MHz, $CDCl_3$, 298 K): δ/ppm = -1.15 (s, S-BINAP). HRMS (ESI): m/z [M]+ for $C_{54}H_{41}CuN_3P_2$: Calculated = 856.2066, Found = 856.2133.

Complex C5: Isolated as bright red powder in 85 % yield (971.9 mg, 1.12 mmol). ^1H NMR (400 MHz, $CDCl_3$, 298 K): δ/ppm = 8.97 (s,1H, N-H), 7.73 (dd, J = 5.6 Hz, 1.8 Hz, 2H), 7.55 (t, *J* = 7.5 Hz, 2H), 7.40 (m, 2H), 7.38–7.2 (m, 20 H), 6.61 (t, *J* = 6.3 Hz), 4.52 (s, 4H), 4.27 (s, 4H). $^{13}C\{^1H\}$ NMR (100 MHz, $CDCl_3$, 298 K): δ/ppm = 154.5, 147.68, 139.16, 133.48, 133.33, 133.17, 133.09, 133.01, 130.16, 128.91, 128.86, 128.82, 117.22, 116.27, 76.31(t, J^{C-P} = 19.1 Hz), 74.24, 72.30. ^{19}F NMR (400 MHz, $CDCl_3$, 298 K): δ/ppm = -151.34 (s, BF_4). ^{11}B NMR (128 MHz, $CDCl_3$, 298 K): δ/ppm = -0.96 (s, BF_4). $^{31}P(^1H)$ NMR (160 MHz, $CDCl_3$, 298 K): δ/ppm = -13.87 (s, dppf). HRMS (ESI): m/z [M]+ for $C_{44}H_{37}CuFeN_3P_2$: Calculated = 788.1108, Found = 788.1164.

4.2. General procedures for the photocatalytic studies

ATRA test reaction: A 10.0 mL flame-dried Schlenk tube with magnetic stirring bar was charged with CBr_4 (0.5 mmol), copper catalyst (1 mol%), and 3 mL of CH_3CN anhydrous solvent, sealed with a screwcap and subsequently degassed by three consecutive freeze-pump-thaw cycles. Afterward, alkene (0.5 mmol) was added under N_2, and the screwcap was replaced with a Teflon sealed inlet for a glass rod, through which irradiation with LED (455 nm) took place from above. At the same time, the reaction mixture was magnetically stirred at 20 °C for 24 h. The reaction was monitored by TLC. Then, the volatiles were removed, and the crude concentrated. The residue was purified by flash chromatography on silica gel (eluent hexanes/ethyl acetate, 9:1).

Chlorosulfonylation reaction over alkene: A 10.0 mL flame-dried Schlenk tube with magnetic stirring bar was charged with TsCl (0.5 mmol), [Cu(dpa)(S-BINAP)]BF_4 (1 mol%), and 3 mL of CH_3CN:CH_2Cl_2 (1.5 mL: 1.5 mL) anhydrous solvent, sealed with a screwcap and subsequently degassed by three consecutive freeze-pump-thaw cycles. Afterward, alkene (0.5 mmol) was added under N_2, and the screwcap was replaced with a Teflon sealed inlet for a glass rod, through which irradiation with LED (455 nm) took place from above. At the same time, the reaction mixture was magnetically stirred at 20 °C for 24 h. The reaction was monitored by TLC. Then, the volatiles were removed, and the crude concentrated. The residue was purified by flash chromatography on silica gel (eluent hexanes/ethyl acetate, 9:1).

Chlorosulfonylation reaction over alkyne: A 10.0 mL flame-dried Schlenk tube with magnetic stirring bar was charged with TsCl derivative (0.5 mmol), [Cu(dpa)(S-BINAP)]BF_4 (2.5 mol%), Na_2CO_3 (1.5 equiv), and 3 mL of CH_3CN:CH_2Cl_2 (1.5 mL: 1.5 mL) anhydrous solvent, sealed with a screwcap and subsequently degassed by three consecutive freeze-pump-thaw cycles. Afterward, alkyne (0.5 mmol) was added under N_2, and the screwcap was replaced with a Teflon sealed inlet for a glass rod, through which irradiation with LED (455 nm) took place from above. At the same time, the reaction mixture was magnetically stirred at 20 °C for 24 h. The reaction was monitored by TLC. Then, the volatiles were removed, and the crude concentrated. The residue was purified by flash chromatography on silica gel (eluent hexanes/ethyl acetate, 5:1).

Appel-type reaction: A 10.0 mL flame-dried Schlenk tube with magnetic stirring bar was charged with tetrabromomethane (2) (331.6 mg, 1.0 mmol, 2.0 equiv), sodium bromide (102.9 mg, 1.0 mmol, 2.0 equiv), [Cu(dpa)(S-BINAP)]BF_4 (2.0 mol%) and dissolved in anhydrous DMF (3.0 mL, 0.17 M), sealed with a screw-cap

and subsequently degassed by three consecutive freeze- pump-thaw cycles. Afterwards, 1-phenylethan-1-ol (8) (61.1 mg, 0.5 mmol, 1.0 equiv) was added under N_2, and the screwcap was replaced with a Teflon sealed inlet for a glass rod, through which irradiation with LED (455 nm) took place from above. At the same time, the reaction mixture was magnetically stirred at 20 °C for 24 h. The reaction was monitored by TLC. Afterwards, the reaction mixture was quenched by addition of water (10 mL) and diethyl ether (10 mL). The layers were separated, and the aqueous phase was extracted with diethyl ether (2x 10 mL). The combined organic layers were washed with saturated $Na_2S_2O_3$ solution (10 mL), brine (10 mL), dried over anhydrous Na_2SO_4 and concentrated in vacuum. The residue was purified by flash column chromatography on silica gel (hexanes).

Decarboxylative coupling reaction: A 10.0 mL flame-dried Schlenk tube with magnetic stirring bar was charged with 1,3- dioxoisoindolin-2-yl cyclohexanecarboxylate[12, 30] (10) (136.6 mg, 0.5 mmol, 1.0 equiv), Hantzsch ester (190.0 mg, 0.75 mmol, 1.5 equiv), [Cu(dpa)(S-BINAP)]BF_4 (2.0 mol%) and dissolved in anhydrous THF (1.5 mL, 0.33 M), sealed with a screw-cap and subsequently degassed by three consecutive freeze-pump-thaw cycles. Afterwards, diisopropylethylamine (129.3 mg, 1.0 mmol, 2.0 equiv) (bromoethynyl)benzene[12, 31] (12) (135.8 mg, 0.75 mmol, 1.5 equiv) were added under N_2, and the screwcap was replaced with a Teflon sealed inlet for a glass rod, through which irradiation with LED (455 nm) took place from above. At the same time, the reaction mixture was magnetically stirred at 20 °C for 24 h. The reaction was monitored by TLC. Afterwards, Then, the volatiles were removed, and the crude concentrated. The residue was purified by flash chromatography on silica gel using as eluent hexanes.

4.3. Computational details

Fully relaxed geometry for all complexes in their ground states was carried out using the Grimme's dispersion corrected (D3)[32] hybrid B3LYP[33] functional (i.e., B3LYP-D3) combined with Def2SVPP double-ζ basis set. The implicit solvent effect was also taken into account in this procedure by the integral equation formalism of the polarizable continuum model (IEFPCM)[34] using acetonitrile as solvent. All structures were confirmed as minima through the harmonic vibrational frequency calculations. The (IEFPCM)-B3LYP-D3/Def2SVPP equilibrium structure has been used to compute vertical excited-states properties within the time-dependent density functional theory (TD-DFT) formalism at the level of theory. For this purpose, a non-equilibrium protocol for solvation was employed to compute vertical excitation energies and oscillator strengths of electronic transitions. All calculations have been performed using Gaussian 09 suite of programs.[35]

Acknowledgements

We gratefully acknowledge the financial support from FONDECYT grant 1210661, Fundamental research project DIPOG 3913-406-81, FONDEQUIP program EQM 160042, EQM 120021, EQM 130021, EQM 180024. M. Henriquez acknowledges Ph.D. CONICYT fellowship 21180705 and *iPUR* program. M. N. gratefully acknowledges the University of Ferrara for funding (FAR2020). I.G.P acknowledges ONR grant N62909-18-1-2180 and FONDECYT 11180185. S. Engl thanks the Studienstiftung des Deutschen Volkes and the Elite Network of Bavaria.

Conflict of Interest

The authors declare no conflict of interest.

Keywords: Chlorosulfonylation • Copper(I) • Dipyridylamine • Heteroleptic • Photocatalysis

[1] Y. S. Kurniawan, K. T. A. Priyangga, P. A. Krisbiantoro, A. C. Imawan, *J. Multidiscip. Appl. Nat. Sci.* **2021**, *1*, 1–12.
[2] D. M. Schultz, T. P. Yoon, *Science* **2014**, *343*, 1239176.
[3] a) C. K. Prier, D. A. Rankic, D. W. MacMillan, *Chem. Rev.* **2013**, *113*, 5322–5363; b) T. P. Yoon, M. A. Ischay, J. Du, *Nat. Chem.* **2010**, *2*, 527–532; c) L. Marzo, S. K. Pagire, O. Reiser, B. König, *Angew. Chem. Int. Ed.* **2018**, *57*, 10034–10072.
[4] N. Armaroli, G. Accorsi, M. Holler, O. Moudam, J. F. Nierengarten, Z. Zhou, R. T. Wegh, R. Welter, *Adv. Mater.* **2006**, *18*, 1313–1316.
[5] a) H. Yersin, R. Czerwieniec, M. Shafikov, A. Suleymanova, *ChemPhysChem* **2017**, *18*, 3508–3535; b) E. Fresta, M. Weber, J. Fernandez-Cestau, R. D. Costa, *Adv. Optical Mater.* **2019**, *7*, 1900830; c) B. M. Hockin, C. Li, N. Robertson, E. Zysman-Colman, *Catal. Sci. Technol.* **2019**, *9*, 889–915.
[6] a) A. Hossain, A. Bhattacharyya, O. Reiser, *Science* **2019**, *364*, eaav9713; b) Y. Abderrazak, A. Bhattacharyya, O. Reiser, *Angew. Chem. Int. Ed.* **2021**, *10.1002/anie.202100270*; c) T. P. Nicholls, A. C. Bissember, *Tetrahedron Lett.* **2019**, *60*, 150883; d) M. Zhong, X. Pannecoucke, P. Jubault, T. Poisson, *Beilstein J. Org. Chem.* **2020**, *16*, 451–481.
[7] J.-M. Kern, J.-P.-. Sauvage, *J. Chem. Soc., Chem. Commun.* **1987**, 546–548.
[8] a) D. B. Bagal, G. Kachkovskyi, M. Knorn, T. Rawner, B. M. Bhanage, O. Reiser, *Angew. Chem. Int. Ed.* **2015**, *54*, 6999–7002; b) T. Rawner, M. Knorn, E. Lutsker, A. Hossain, O. Reiser, *J. Org. Chem.* **2016**, *81*, 7139–7147; c) A. Hossain, S. Engl, E. Lutsker, O. Reiser, *ACS Catal.* **2019**, *9*, 1103−1109; d) S. Paria, M. Pirtsch, V. Kais, O. Reiser, *Synthesis* **2013**, *45*, 2689–2698; e) X.-J. Tang, W. R. Dolbier Jr., *Angew. Chem. Int. Ed.* **2015**, *54*, 4246–4249; f) P. T. G. Rabet, G. Fumagalli, S. Boyd, M. F. Greaney, *Org. Lett.* **2016**, *18*, 1646–1649; g) T. Rawner, E. Lutsker, C. A. Kaiser, O. Reiser, *ACS Catal.* **2018**, *8*, 3950–3956; h) C. O. Dietrich-Buchecker, P. A. Marnot, J. P. Sauvage, J. P. Kintzinger, P. Maltese, *Nouv. J. Chim.* **1984**, *8*, 573–582; i) M. Pirtsch, S. Paria, T. Matsuno, H. Isobe, O. Reiser, *Chem. - Eur. J.* **2012**, *18*, 7336–7340; j) S. Engl, O. Reiser, *ACS Catal.* **2020**, *10*, 9899–9906.
[9] S. Engl, O. Reiser, *Eur. J. Org. Chem* **2020**, 1523–1533.
[10] a) A. C. Hernandez-Perez, S. K. Collins, *Acc. Chem. Res.* **2016**, *49*, 1557–1565; b) S. P. Luo, E. Mejia, A. Friedrich, A. Pazidis, H. Junge, A. E. Surkus, R. Jackstell, S. Denurra, S. Gladiali, S. Lochbrunner, M. Beller, *Angew. Chem. Int. Ed. Engl.* **2013**, *52*, 419-423; c) H. Chen, L.-X. Xu, L.-J. Yan, X.-F. Liu, D.-D. Xu, X.-C. Yu, J.-X. Fan, Q.-A. Wu, S.-P. Luo, *Dyes Pigm.* **2020**, *173*, 108000.
[11] a) K. Saito, T. Arai, N. Takahashi, T. Tsukuda, T. Tsubomura, *Dalton Trans.* **2006**, *37*, 4444–4448; b) M. Iwamura, S. Takeuchi, T. Tahara, *Phys. Chem. Chem. Phys.* **2014**, *16*, 4143–4154.
[12] C. Minozzi, A. Caron, J.-C. Grenier-Petel, J. Santandrea, S. C. Collins, *Angew. Chem. Int. Ed.* **2018**, *57*, 5477–5481.
[13] C. Minozzi, J.-C. Grenier-Petel, S. Parisien-Collette, S. K. Collins, *Beilstein J. Org. Chem.* **2018**, *14*, 2730–2736.
[14] a) M. Knorn, T. Rawner, R. Czerwieniec, O. Reiser, *ACS Catal.* **2015**, *5*, 5186–5193; b) B. Wang, D. P. Shelar, X.-Z. Han, T.-T. Li, X. Guan, W. Lu, K. Liu, Y. Chen, W. F. Fu, C.-M. Che, *Chem. - Eur. J.* **2015**, *21*, 1184–1190 ; c) C. J. Hunter, M. J. Boyd, G. D. May, R. Fimognari, *J. Org. Chem.* **2020**, *85*, 8732–8739; d) A. Caron, É. Morin, S. K. Collins, *ACS Catal.* **2019**, *9*, 9458–9464; e) M. Alkan-Zambada, X. Hu, *Organometallics* **2018**, *37*, 3928–3935.
[15] a) A. R. Cabrera, I. A. González, D. Cortés-A., M. Natali, H. Berke, C. G. Daniliuc, M. B. Camarada, A. Toro-L., R. S. Rojas, C. O. Salas, *RSC Adv.* **2016**, *6*, 5141–5153; b) I. A. González, Henríquez, M.A., D. Cortés-Arriagada, M. Natali, C. G. Daniliuc, P. Dreyse, J. Maze, R. S. Rojas, C. O. Salas, A. R. Cabrera, *New J. Chem.* **2018**, *42*, 12576–12586; c) M. A. Escobar, C. Morales-Verdejo, J. L. Arroyo, P. Dreyse, I. Gonzalez, I. Brito, D. MacLeod-Carey, D. Moreno da Costa, A. R. Cabrera, *Eur. J. Inorg. Chem* **2021**, 1632–1639
[16] M. Elie, F. Sguerra, F. Di Meo, M. D. Weber, R. Marion, A. Grimault, J.-F. Lohier, A. Stallivieri, A. Brosseau, R. B. Pansu, J.-L. Renaud, M. Linares, M. Hamel, R. D. Costa, S. Gaillard, *ACS Appl. Mater. Interfaces* **2016**, *8*, 14678–14691.
[17] E. Leoni, J. Mohanraj, M. Holler, M. Mohankumar, I. Nierengarten, F. Monti, A. Sournia-Saquet, B. Delavaux-Nicot, J.-F. Nierengarten, N. Armaroli, *Inorg. Chem.* **2018**, *57*, 15537–15549.
[18] A. Kaeser, M. Mohankumar, J. Mohanraj, F. Monti, M. Holler, J.-J. Cid, O. Moudam, I. Nierengarten, L. Karmazin-Brelot, C. Duhayon, B. Delavaux-Nicot, N. Armaroli, J.-F. Nierengarten, *Inorg. Chem.* **2013**, *52*, 12140–12151.
[19] a) N. Armaroli, G. Accorsi, G. Bergamini, P. Ceroni, M. Holler, O. Moudam, C. Duhayon, B. Delavaux-Nicot, J.-F. Nierengarten, *Inorg. Chim. Acta* **2007**, *360*, 1032–1042; b) A. Listorti, G. Accorsi, Y. Rio, N. Armaroli, O. Moudam, A. Gégout, B. Delavaux-Nicot, M. Holler, J.-F. Nierengarten, *Inorg. Chem.* **2008**, *47*, 6254–6261.
[20] T. McCormick, W.-L. Jia, S. Wang, *Inorg. Chem.* **2006**, *45*, 147–155.
[21] Y. Zhang, M. Schulz, M. Wächtler, M. Karnahl, B. Dietzek, *Coord. Chem. Rev.* **2018**, *356*, 127–146.
[22] H. Kunkely, V. Pawlowski, A. Vogler, *Inorg. Chem. Commun.* **2008**, *11*, 1003–1005.
[23] M. Alkan-Zambada, X. Hu, *J. Org. Chem.* **2019**, *84*, 4525–4533.
[24] C. Cruché, W. Neiderer, S. K. Collins, *ACS Catal.* **2021**, *11*, 8829–8836.
[25] a) S. K. Parida, T. Mandal, S. Das, S. K. Hota, S. D. Sarkar, S. Murarka, *ACS Catal.* **2021**, *11*, 1640−1683; b) W. Zhao, R. P. Wurz, J. C. Peters, G. C. Fu, *J. Am. Chem. Soc.* **2017**, *139*, 12153–12156; c) C. Wang, M. Guo, R. Qi, Q. Shang, Q. Liu, S. Wang, L. Zhao, R. X. Wang, Z. , *Angew. Chem., Int. Ed.* **2018**, *57*, 15841–15846; d) Y. Mao, W. Zhao, S. Lu, L. Yu, Y. Wang, Y. Liang, S. Ni, Y. Pan *Chem. Sci.* **2020**, *11*, 4939–4947.
[26] D. S. Patil, K. K. Sonigara, M. M. Jadhav, K. C. Avhad, S. Sharma, S. S. Soni, N. Sekar, *New J. Chem.* **2018**, *42*, 4361–4371.
[27] G. M. Sheldrick, *Acta Crystallogr., Sect. A: Found. Adv.* **2015**, *71*, 3−8.
[28] O. V. Dolomanov, L. J. Bourhis, R. J. Gildea, J. A. K. Howard, H. Puschmann, *J. Appl. Crystallogr.* **2009**, *42*, 339−341.
[29] G. M. Sheldrick, *Acta Crystallogr., Sect. C: Struct. Chem.* **2015**, *71*, 3−8.
[30] J. Cornella, J. T. Edwards, T. Qin, S. Kawamura, J. Wang, C.-M. Pan, R. Gianatassio, M. Schmidt, M. D. Eastgate, P. S. Baran, *J. Am. Chem. Soc.* **2016**, *138*, 2174−2177.
[31] J. Yang, J. Zhang, L. Qi, C. Hu, Y. Chen, *Chem. Commun.* **2015**, *51*, 5275−5278.
[32] S. Grimme, J. Antony, S. Ehrlich, H. Krieg, *J. Chem. Phys.* **2010**, *132*, 154104.
[33] a) A. D. Becke, *J. Chem. Phys.* **1993**, *98*, 5648–5652; b) A. D. Becke, *Phys. Rev. A* **1988**, *38*, 3098; c) S. H. Vosko, L. Wilk, M. Nusair, *Can. J. Phys.* **1980**, *58*, 1200–1211; d) P. J. Stephens, F. J. Devlin, C. F. Chabalowski, M. J. Frisch, *J. Phys. Chem. B* **1994**, *98*, 11623–11627; e) C. Lee, W. Yang, R. G. Parr, *Phys. Rev. B* **1988**, *37*, 785–789.
[34] B. Mennucci, C. Cappelli, C. A. Guido, R. Cammi, J. Tomasi, *J. Phys. Chem. A* **2009**, *113*, 3009–3020.

[35] M. J. Frisch, G. W. Trucks, H. B. Schlegel, G. E. Scuseria, M. A. Robb, J. R. Cheeseman, G. Scalmani, V. Barone, B. Mennucci, G. A. Petersson, *et al.*, *Gaussian 09 Rev. B.01, Gaussian Inc., Wallingford, CT,* **2009**.